Atmospheric Pollution Research 5 (2014) 210-218

Atmospheric Pollution Research

www.atmospolres.com

Phase distribution, sources and risk assessment of PAHs, NPAHs and OPAHs in a rural site of Pearl River Delta region, China

Bo Huang [1,2], Ming Liu [1,2], Xinhui Bi [1], Chakra Chaemfa [1], Zhaofang Ren [1,2], Xinming Wang [1], Guoying Sheng [1], Jiamo Fu [1,3]

[1] *State Key Laboratory of Organic Geochemistry, Guangdong Province Key Laboratory of Utilization and Protection of Environmental Resource, Guangzhou Institute of Geochemistry, Chinese Academy of Sciences, Guangzhou 510640, P.R. China*
[2] *Graduate University of Chinese Academy of Sciences, Beijing 100049, P. R. China*
[3] *School of Environmental and Chemical Engineering, Shanghai University, Shanghai 200444, P. R. China*

ABSTRACT

Gaseous and particulate samples were collected in the late autumn of 2010 from Wanqingsha (WQS), a rural site in the Pearl River Delta (PRD) region, China. Eighteen polycyclic aromatic hydrocarbons (PAHs), twenty–nine nitrated PAHs (NPAHs) and six oxygenated PAHs (OPAHs) were measured, and their gas–particle partitioning, sources and risks were discussed. The results showed that the atmospheric mass distribution was dominated by three and four rings compounds. Phenanthrene, 2–nitrofluoranthene and benzanthrone were the most abundant parent PAH, NPAH and OPAH, respectively. The partitioning of these compounds was strongly dependent on their molecular weights. The absorption model provides a better prediction of the particulate fraction of PAHs than the adsorption model, and might be applied for the discrimination of PAH derivatives sources. Molecular diagnostic ratios suggested that coal combustion or biomass burning, not vehicle emission, were the dominant sources in WQS. The ratios of 2–nitrofluoranthene/2–nitropyrene and 2–nirtofluoranthene/1–nitropyrene indicated that secondary formation by OH initiated reactions was the main formation pathway for NPAHs, with an average contribution of 92.6% during the sampling period, and the formation might be enhanced under hazy conditions. Most of OPAHs were under the impact of regional pollution. Risk assessment showed an overall lifetime excess inhalation cancer risk of 1.12×10^{-5} in which the six NPAHs taken into calculation contributed 3.5% although they only accounted for 0.7% of the 18 compound masses used in the assessment.

Keywords: *Nitrated PAHs, oxygenated PAHs, gas–particle partitioning, source apportionment, risk assessment*

Corresponding Author:
Xinhui Bi
☎ : *+86-20-85290195*
🖷 : *+86-20-85290288*
✉ : *bixh@gig.ac.cn*

Article History:
Received: 17 July 2013
Revised: 15 December 2013
Accepted: 16 December 2013

doi: 10.5094/APR.2014.026

1. Introduction

Polycyclic aromatic hydrocarbons (PAHs) are a series of harmful compounds emitted into the environment through natural or anthropogenic processes (Ravindra et al., 2008). They are of great concern because of their known mutagenic and carcinogenic properties (IARC, 2012). During the last decade, research interest has moved to PAH derivatives, such as nitrated PAHs (NPAHs) and oxygenated PAHs (OPAHs). These derivatives are more toxic than their parent PAHs due to their direct–acting mutagenicity and carcinogenicity (EHC, 2003), and could be important contributors to the high toxicity of particles at extremely low levels (Kawanaka et al., 2008). Some OPAHs, such as polycyclic aromatic quinones, could generate reactive oxygen species that result in oxidative stress leading to allergic diseases (Sklorz et al., 2007). Additionally, OPAHs have been subjected as "dead–end products" of many biological and chemical degradation pathways (Lundstedt et al., 2007), making them more persistent in the environment.

Both PAHs and their derivatives are semi– to low–volatile pollutants. The transport, chemical transformation, and fate of these compounds are influenced by their gas–particle partitioning (Bidleman, 1988; Cotham and Bidleman, 1995). Also, the degradation and deposition of these compounds in the human respiratory tract strongly depends on their existence in the gaseous and particulate phases (Pankow, 2001; Lohmann and Lammel, 2004). The gas–particle partitioning of PAHs have been extensively studied (Bi et al., 2003; Odabasi et al., 2006), however, limited research has been conducted on NPAHs and OPAHs (Wilson and Mccurdy, 1995; Albinet et al., 2007; Albinet et al., 2008). Therefore, more studies of the PAH derivatives are needed in order to gain knowledge on their source, fate, distribution and transportation.

The Pearl River Delta (PRD) region, covering Guangzhou, Hong Kong and several mid–size cities, is one of the most populated areas in China. During the last few decades, rapid growth in urbanization and industrialization has caused many severe environmental pollution issues, for example, high levels of PAHs in the atmosphere (Bi et al., 2003). In this study, the gaseous and particulate concentrations of PAHs, NPAHs and OPAHs at a rural site in PRD region measured during the late autumn of 2010 were investigated. The levels, gas–particle partitioning, potential sources and risks of these target compounds were also discussed. The results are expected to provide a better understanding on PAHs, NPAHs and OPAHs sources and their transformation mechanisms during transport.

2. Material and Methods

2.1. Sample collection

The atmospheric condition of the PRD region is strongly influenced by the Asian monsoon system. The southwesterly to southeasterly monsoon brings relatively clean air from the sea in summer and spring, and northeasterly wind carries relatively polluted air masses across northern cities in fall and winter (Tan et al., 2009). In order to monitor the influence of inner PRD on the sampling site, sample acquisition was carried out from November 4 to December 6, 2010, when most of winds were from the northeast [see the Supporting Material (SM), Figure S1]. The sampling site Wanqingsha (WQS) (22.712°N, 113.549°E) is a small town situated at the mouth of Pearl River Estuary, which is approximately at the center of the PRD region (Figure 1). It is surrounded by the city cluster of PRD, with the distances to Guangzhou, Shenzhen, Zhuhai, Hong Kong, and Macao all being within about 60 km. Samples were collected on the rooftop of a 15 m high building in Wanqingsha Middle School. The influence of anthropogenic activities is limited due to the sparse emission sources. There is only a coal–fired electric power plant, about 10 km north of the sampling location (also in the upwind direction of the site during the sampling period), which could account for the local emissions.

A high–volume air sampler was deployed at a flow rate of about 300 L min^{-1}. Samples were collected every day and every sampling period lasted for approximate 24 h. Particulate and gaseous contaminants were collected on quartz fiber filters (QFFs, 20.3 cm × 25.4 cm, Whatman) and polyurethane foams (PUF, 6.5 cm diameter × 8 cm), respectively. PUF breakthrough was not tested in this study. However, it should not be a problem because it would only affect those most volatile compounds such as fluorene (Fl) and acenaphthylene (Acy). The backup PUF contained only a small portion of the vapor phase component according to previous studies by of our group (Bi et al., 2003; Chen et al., 2004), and with larger molecular weights, the possibility of breakthrough becomes really small for NPAHs and OPAHs. Prior to the sampling, QFFs were baked at 450 °C for 6 hours to remove any potential organic contamination and then stored in aluminum foil packages until they were deployed. PUFs were Soxhlet extracted with dichloromethane (DCM) for 72 h and dried under vacuum. After the sampling, the exposed filters were wrapped with pre–baked aluminum foils and placed in sealed bags. Concentration of total suspended particles (TSP) was determined by weighing the filters before and after the sampling (see the SM, Table S2) under controlled temperature and moisture [25 °C, 50% relative humidity (RH)] in a separated room. After weighing, the samples were stored in a freezer at –40 °C till analysis. In total, 32 pairs of particulate (GFFs) and gaseous (PUFs) samples were collected.

Because of an instrumental failure (Trace Gases series, Thermo Scientific, USA), concentrations of trace gases, such as NO, NO_X, O_3 and SO_2 were only recorded during the latter half of the sampling period. Meteorological parameters like temperature, RH, wind speed, wind direction and solar radiation were measured by a mini weather station (Davis Advantage Professional 2). The trace gas concentrations and meteorological conditions are presented in Table S2 (see the SM).

2.2. Analytical procedure

A detailed description of the analytical protocol has been published elsewhere (Wei et al., 2012). Briefly, five PAHs surrogates (naphthalene–D_8, acenaphthylene–D_{10}, phenanthrene–D_{10}, chrysene–D_{12}, perylene–D_{12}) and four NPAHs surrogates, (5–nitroacenaphthene–D_9, 9–nitroanthracene–D_9, 3–nitrofluoranthene–D_9, 6–nitrochrysene–D_{11}) were added into the samples prior to extraction. Then, the filters were ultrasonically extracted with DCM for 30 min and repeated 3 times. PUFs were Soxhlet extracted with DCM for 48 h. The extracts were filtered in order to remove filter debris, and then concentrated and cleaned up using 2:1 silica–alumina columns. Two fractions were eluted: Fraction I (eluted with 40 mL of hexane) containing aliphatic hydrocarbons was discarded, while fraction II [eluted with 100 mL of DCM–hexane (1:1)] containing parent PAHs and their derivatives (NPAHs and OPAHs) was collected. The collected fraction (II) was reduced almost to dryness, then dissolved in n–hexane. Internal standards, hexamethylbenzene and 2–nitrofluorene–D_9 were then added for quantification of the parent PAHs and N/OPAHs, respectively.

All samples were analyzed using gas chromatography/mass spectrometry (GC/MS) under selected ion monitoring (SIM) mode. The mass spectrometer was operated in electron impact ionization (EI) mode for parent PAHs, and negative chemical ionization (NICI) mode for NPAHs and OPAHs. A DB–5MS GC column (30 m × 0.25 mm × 0.25 μm) were used to measure parent PAHs and most of NPAHs and OPAHs, and a DB–17MS column (60 m × 0.25 mm × 0.25 μm) were used to separate 2–nitrofluoranthene (2NF) and 3–nitrofluoranthene (3NF). Target compounds were identified based on the retention time and qualitative ions of the standards. Overall, eighteen parent PAHs, twenty–nine NPAHs and six OPAHs were quantified in this study. The compounds list and individual average concentrations in gaseous and particulate phases are presented in Table 1. The carbonaceous species organic carbon (OC) and elemental carbon (EC) were also measured by a Thermal–Optical Carbon Aerosol Analyzer (see the SM, Table S2). The detailed analytical methods and instrumental conditions are provided in the SM.

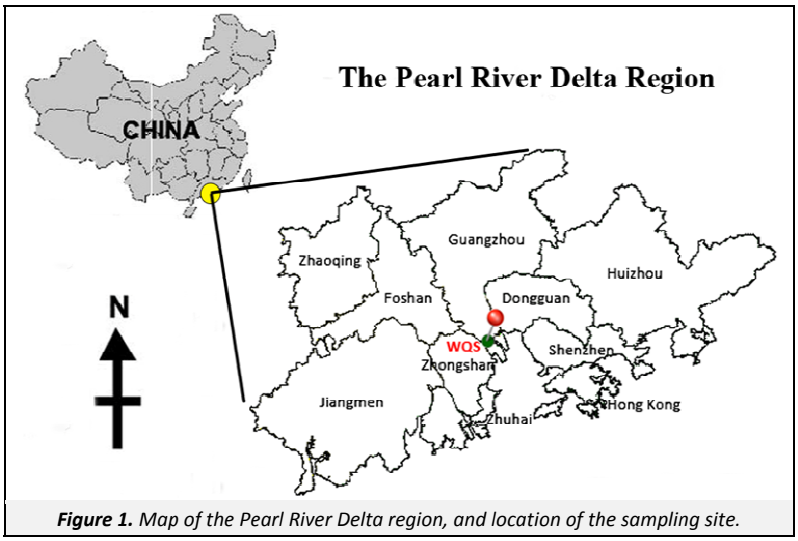

Figure 1. *Map of the Pearl River Delta region, and location of the sampling site.*

Table 1. *Average concentrations of gaseous and particulate PAHs (ng m^{-3}), NPAHs (pg m^{-3}) and OPAHs (ng m^{-3}) in WQS*

		Abbreviation	Number of rings	Concentration		
				Particle (P)	Gas (G)	P+G
PAHs	Acenaphthylene	Acy	3	0.016	1.78	1.8
	Acenaphthene	Ace	3	0.004	0.20	0.21
	Fluorene	Fl	3	0.033	5.76	5.79
	Phenanthrene	Phe	3	0.52	39.5	40
	Anthracene	Ant	3	0.052	1.49	1.54
	Retene	Ret	3	0.25	1.04	1.29
	Fluoranthene	Fla	4	1.61	13	14.6
	Pyrene	Pyr	4	1.62	8.19	9.81
	Benz[a]anthracene	BaA	4	0.93	0.17	1.09
	Chrysene	Chr	4	2.26	0.95	3.21
	1,3,5–Triphenylbenzene	TPB	4	0.72	0.011	0.73
	Benzo[*b*]fluoranthene	BbF	5	3.07	0.082	3.15
	Benzo[*k*]fluoranthene	BkF	5	1.27	0.021	1.29
	Benzo[*a*]pyrene	BaP	5	1.63	0.018	1.65
	Dibenzo[*a,h*]anthrathene	DBahA	5	0.37	0.003	0.37
	Benzo[*g,h,i*]perylene	BghiP	6	2.66	0.011	2.67
	Indeno[1,2-*cd*]pyrene	IcdP	6	2.32	0.012	2.33
	ΣPAHs			19.3	72.2	91.5
NPAHs	1–nitronaphthalene	1NN	2	5.5	311	317
	2–nitronaphthalene	2NN	2	1.91	275	277
	3–nitrobiphenyl	3NBp	2	0.014	2.35	2.37
	4–nitrobiphenyl	4NBp	2	1.01	223	224
	2–nitrobiphenyl	2NBp	2	0.50	12.6	13.1
	1,5–dinitronaphthalene	1,5DNN	2	0.1	0.59	0.69
	1,3–dinitronaphthalene	1,3DNN	2	0.86	1.33	2.19
	1,8–dinitronaphthalene	1,8DNN	2	0.23	0.97	1.19
	3–nitrodibenzofuran	3NDBF	3	1.22	23	24.2
	5–nitroacenaphthene	5NAce	3	0.40	5.43	5.83
	2–nitrofluorene	2NFlo	3	0.17	0.99	1.16
	9–nitroanthracene	9NA	3	779	40.2	820
	2–nitroanthracene	2NA	3	3.96	2.52	6.48
	2–nitrodibenzothiophene	2NDBT	3	2.1	1.19	3.3
	9–nitrophenanthrene	9NPhe	3	19.6	19.4	39
	3–nitrophenanthrene	3NPhe	3	0.68	1.44	2.12
	2,7–dinitrofluorene	DNFl	3	6.65	0.31	6.96
	2,8–dinitrodibenzothiophene	DNDBT	3	32.6	0.27	32.9
	2–nitrofluoranthene	2NF	4	1 548	48.1	1 596
	3–nitrofluoranthene	3NF	4	2.66	0.088	2.75
	1–nitropyrene	1NP	4	16.6	0.39	17
	4–nitropyrene	4NP	4	14.6	0.74	15.3
	2–nitropyrene	2NP	4	106	1.04	107
	7–nitrobenz[a]anthracene	7NBaA	4	527	0.34	527
	6–nitrochrysene	6NChr	4	2.44	0.043	2.48
	1,3–dinitropyrene	1,2DNP	4	13	0.034	13.1
	1,6–dinitropyrene	1,6DNP	4	26.6	0	26.6
	1,8–dinitropyrene	1,8DNP	4	44.6	0	44.6
	6–nitrobenz(a)pyrene	6NBaP	5	63	0	63
	ΣNPAHs			3 173	971	4 143
OPAHs	9–fluorenone	Fluon	3	0.087	2.2	2.29
	Anthraquinone	Anquin	3	1.08	1.43	2.51
	2,7–dinitro–9–fluorenone	DNFluon	3	0.091	0.007	0.097
	cyclopenta[def]phenanthrene–4–one	Cphone	4	0.11	0.43	0.54
	Benzanthrone	Bzone	4	4.81	0.09	4.9
	Benz(a)anthracene–7,12–dione	Bzdion	4	2.68	0.027	2.7
	ΣOPAHs			8.85	4.18	13

2.3. Quality control

Surrogate standards were added to all samples to monitor procedural performance and matrix effects. The mean recoveries for parent PAHs were 15.1% (naphthalene–D_8), 51.8% (acenaphthylene–D_{10}), 116.8% (phenanthrene–D_{10}), 119.2% (chrysene–D_{12}) and 134.6% (perylene–D_{12}). The mean recoveries for NPAHs and OPAHs were 94.2% (5–nitroacenaphthene–D_9), 49.2% (9–nitroanthracene–D_9), 109.2% (3–nitrofluoranthene–D_9) and 98.5% (6–nitrochrysene–D_{11}). Naphthalene (Nap) was not discussed in this study due to the extremely low recovery of naphthalene–D_8 (much less than 50%). One analytical blank was performed every ten samples using field blank samples. Solvent blanks were also analyzed. The major contaminants observed were light parent PAHs Nap and phenanthrene (Phe), and light OPAH 9–fluorenone (Fluon). Generally, these blank levels were below 5% of the measured concentrations in samples. Other compounds were only in trace levels, and NPAHs were not detected.

2.4. Gas/particle partitioning models

The partitioning of PAHs, NPAHs and OPAHs in gaseous and particulate phases can be described using the gas–particle partitioning coefficients (K_p) as follows:

$$K_p=[F]/([TSP][A]) \quad (1)$$

where, [*F*] and [*A*] are concentrations of target compounds in particulate and gaseous phases (ng m^{-3}), and [*TSP*] is the concentration of TSP in the atmosphere (μg m^{-3}) (Yamasaki et al., 1982). The gas–particle partitioning is believed to be governed by adsorption which is more related to the particulate surface area and EC content, or absorption which is associated with the organic matter in particulate matter (Goss and Schwarzenbach, 1998). The Junge–Pankow adsorption and K_{OA}–based absorption models are usually used to predict the particulate fraction (ϕ) of semi–volatile organic compounds (Lohmann and Lammel, 2004; Odabasi et al., 2006). The adsorption model derives ϕ as follows:

$$\phi=c\,S_T/(P_L^0+c\,S_T) \quad (2)$$

where, c=17.2 Pa cm. S_T is the average total surface area of aerosol (cm^2 cm^{-3}), and the value of 3.5×10^{-6} was suggested by Bidleman (1988) for an air regime of the background site plus local sources. P_L^0 is the subcooled liquid vapor pressure (Pa). In this study, temperature dependent P_L^0 of PAHs were obtained from Odabasi et al. (2006). Temperature dependent P_L^0 of major NPAHs and OPAHs were calculated using the SPARC online calculator (SPARC, 2013). The absorption model predicts ϕ as follows (Harner and Bidleman, 1998):

$$\log K_p=\log K_{OA}+\log f_{OM}-11.9 \quad (3)$$

$$\phi=K_p\,TSP/(1+K_p\,TSP) \quad (4)$$

where, K_{OA} is the octanol–air partition coefficient obtained from Odabasi et al. (2006); f_{OM} is the mass fraction of organic matter [OC was multiplied by a factor of 2.1 for the transformation to OM (Turpin and Lim, 2001)]. The K_{OA} values for NPAHs and OPAHs were not available, thus only the partitioning of PAHs were predicted using this model.

3. Results and Discussion

3.1. Concentration levels of PAHs, NPAHs and OPAHs

The total concentration of parent PAHs (ΣPAHs) was 91.5±36.1 ng m^{-3}, while the abundance of ΣNPAHs and ΣOPAHs were approximately one order of magnitude lower, with the average values of 4.14±2.37 ng m^{-3} and 13.0±6.63 ng m^{-3}, respectively (Table 1). The atmospheric mass distribution of the target compounds (including gaseous and particulate phases) was dominated by three and four–ring compounds, accounting for 87.5%, 78.5% and 100% of measured ΣPAHs, ΣNPAHs and ΣOPAHs, respectively.

Among the parent PAHs, phenanthrene (Phe), fluoranthene (Fla), and pyrene (Pyr) were the most abundant. The PAH concentrations measured at WQS were comparable with those detected in the urban sites such as Guangzhou (China) (Bi et al., 2003) and Seoul (Korea) (Kim et al., 2012a), but were higher than other rural or suburban sites, like Gosan (Korea) (Kim et al., 2012b) and Frascati (Italy) (Chirico et al., 2007), and were several times lower than Eskisehir (Turkey) (Gaga and Ari, 2011), Chicago (USA) (Odabasi et al., 1999) and Taichung (Taiwan) (Fang et al., 2004).

Interestingly, NPAHs levels in this study were, to our knowledge, the highest among other similar investigations. The three most abundant NPAHs in this study were 2NF, 9–nitroanthracene (9NA) and 7–nitrobenz[a]anthracene (7NBaA), consisting of 38.5%, 19.8% and 12.7% of ΣNPAHs, respectively. A further discussion is given in Section 3.3.

The concentration of Benzanthrone (Bzone) was the highest among measured OPAHs in this study, taking up 37.6% of total OPAHs. The OPAH levels were similar to those in Maurienne valley (France) (Albinet et al., 2008), Tokyo (Japan) (Kojima et al., 2010) and Providencia (Chile) (Sienra and Rosazza, 2006), but higher than those in Athens (Greece) (Andreou and Rapsomanikis, 2009), Qingyuan (China) (Wei et al., 2012) and Las Condes (Chile) (Sienra and Rosazza, 2006).

3.2. Gas–particle partitioning

Gas–particle partitioning is an important process that controls the transport, degradation, and fate of organic contaminants in the environment. The partitioning of PAHs, NPAHs and OPAHs are strongly dependent on their molecular weight (MW) (Odabasi et al., 1999; Albinet et al., 2008). As shown in Figure S2 (see the SM), the mass fraction for the particulate phase showed an increasing trend proportional to MW, which was quite similar with the findings of Albinet et al. (2008). Particulate mass fractions of compounds with MW<202 were less than 20%, while those of compounds with MW>229 were over 90%. The influence of temperature variability on the partitioning of the compounds of interest was also explored, however, due to the narrow temperature range during the sampling period (21.7±1.2 °C), no significant correlation was found between the particulate fraction of the target compounds and temperature. The most abundant compounds for the particulate phase were benzo[*b*]fluoranthene (BbF), 2NF and Bzone, which constituted 15.9%, 48.8% and 54.4% of the total PAHs, NPAHs and OPAHs particulate phase concentrations, respectively. With few anthropogenic activities around the sampling site, concentrations of PAHs and their derivatives were expected to be influenced by long–range transport (LRT) of air masses from surrounding cities. The average wind speed during the whole sampling period was 1.44 m s^{-1}, and it would take about 12 h for the air masses from surrounding cities to reach to the sampling site. The atmospheric residence times could be sufficient to allow most of these compounds to reach equilibrium state (Simcik et al., 1998).

Figure 2 compares the measured particulate fractions of PAHs, NPAHs and OPAHs with predicted values obtained from the adsorption model or absorption model. Both models underestimated the particulate fractions of PAHs, and a similar trend was found for some NPAHs and OPAHs (such as 1NP, 9NA, 9–fluorenone and Bzone) which were reported to be primarily emitted compounds (Albinet et al., 2007). In our recent studies on coal combustion and vehicle emissions, Fluon and Bzone were found to be the most abundant OPAHs measured in coal combustion and vehicle emissions, respectively (unpublished data).

The discrepancy between measured and predicted values might be caused by the presence of non–exchangeable fractions (Callen et al., 2008). Being trapped in the particles during combustion, these PAHs are not thermodynamically active, and are not able to participate in the gas–particle exchange, resulting in high fractions in the particulate phase. Another cause could be attributed to artifacts during sampling, with the existence of PUF breakthrough, the measured particulate fractions for lighter compounds were larger than they should be. However, the gas–particle partitioning of some NPAHs and OPAHs like 2NF, 9–nitrophenanthrene (9NPhe), anthraquinone (Anquin) and benz(a)anthracene–7,12–dione (Bzdion), whose concentrations could be attributed to secondary formation (Bamford and Baker, 2003; Ringuet et al., 2012), showed a different pattern, and the predicted particulate fractions were somehow overestimated. A possible explanation was that with rapid transformation rates in the gaseous phase, these compounds were not able to reach the equilibrium state, resulting in higher concentrations in the gaseous phase. However, the particulate fraction of 2–nitropyrene (2NP), which was also reported to be mainly secondarily formed (Arey et al., 1986), was underestimated by the adsorption model. This was possible due to the significant formation of 2NP by the heterogeneous reaction of Pyr in particulate phase (Ringuet et al., 2012). These results implied that the gas–particle partitioning models may be used as an assistive tool to distinguish the main sources of PAH derivatives: primary sources or gas–phase secondary reaction sources (not valid if heterogeneous formation is significant).

The relationship between particulate phase PAH species with OC and EC was analyzed. The results showed similar correlations between most species with OC and EC (see the SM, Table S3), indicating that both mechanisms might be important during the partitioning. For PAHs, the particulate fraction values obtained from the absorption were closer to the measured results than the adsorption model. This also agrees with the finding of Goss and Schwarzenbach (1998), which reported that sorption from gas to particles for the organic compounds is mainly governed by absorption.

3.3. Source identification

Correlation with trace gases. The relationship between target compounds (total gaseous and particulate concentrations were used) and trace gases could give us some information about their origins. The correlations are presented in Table S4 (see the SM).

Positive correlations with NO and NO_X were observed for almost all of the parent PAHs, most of NPAHs and one OPAH (DNFluon). NO is a short–lived species, and is accepted as a good tracer for close traffic (Janhall et al., 2004). Correlations with NO_X may reflect the formation of nitro–compounds through direct reactions with NO_X or oxidants that co–vary with NO_X in the atmosphere (Bamford and Baker, 2003). In this study, strong correlation was found between NO and NO_X (R=0.902, p<0.01), therefore, we cannot distinguish primary sources from secondary pathways for those compounds by these correlation analyses.

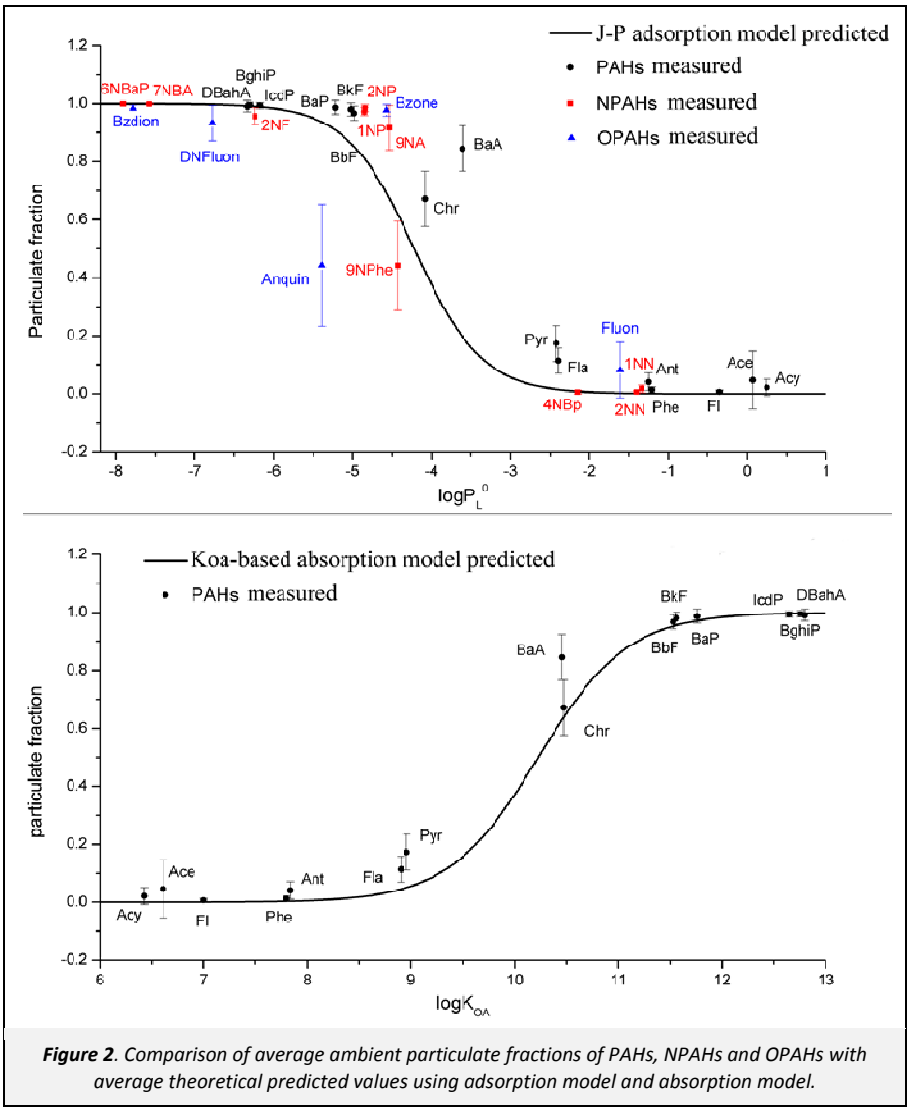

***Figure 2**. Comparison of average ambient particulate fractions of PAHs, NPAHs and OPAHs with average theoretical predicted values using adsorption model and absorption model.*

Due to the unique geographical location of the sampling site, the continuous inflow of air masses from the surrounding cities of PRD might significantly contribute to the atmospheric concentrations of PAHs and their derivatives in WQS. 2NF, mostly produced from the gaseous reaction (Arey et al., 1986; Atkinson et al., 1987), showed much higher concentrations than any other similar investigations, which might be the results of enhanced secondary formation due to the atmospheric LRT. The atmospheric lifetime of SO_2 is about 10 days (ATSDR, 1998), making it an acceptable tracer for the evaluation of LRT. Positive correlations with SO_2 were observed for most of parent PAHs, OPAHs and some of NPAHs. These correlations implied that many of our monitored compounds were under the influence of LRT.

Negative correlations with O_3 for most of target compounds were found except for several NPAHs such as 1–nitronaphthalene (1NN), 2–nitronaphthalene (2NN), 4–nitrobiphenyl (4NBp), 3–nitrodibenzofuran (3NDBF), 2–nitroanthracene (2NA) and 6–nitrochrysene (6NChr), these compounds were found to be positively correlated with O_3. The negative correlations with O_3, although not statistically significant, could reflect the loss process of compounds through reactions with O_3 (Fan et al., 1996). The positive correlations with O_3 may suggest different formation pathways of these compounds, e.g. heterogeneous nitration of parent compounds when exposing to O_3 and NO_2 (Bamford and Baker, 2003).

PAHs sources. Molecular diagnostic ratios have been widely used to investigate PAHs sources (Tobiszewski and Namiesnik, 2012). As most of source profiles were only available for particulate phase composition, we focused on the variances of IcdP and BghiP which mainly reside in the particulate phase.

Figure 3a displays the scatter plots of BghiP versus IcdP. The significant deviation of the ambient line from vehicular source profile indicates that vehicular emission was not the dominant source in WQS. Figure 3b displays the ratio–to–ratio plot of the two PAHs normalized by EC, along with normalized ratios for gasoline and diesel emission (Watson et al., 1998), Zhujiang Tunnel 2004 (He et al., 2008), Zhujiang Tunnel 2012 (unpublished results), industrial coal combustion (Zhang et al., 2008), and biomass burning in Guangzhou (Wang, 2008). The ratio–to–ratio plot visualizes ambient data and source profiles more clear, and could also reflect the photochemical oxidation of PAHs by atmospheric oxide species: photochemical decay will result in a linear distribution of ambient data from the source profile to the lower left corner of the plot (Robinson et al., 2006). It seems that the dominance of industrial coal combustion or biomass burning in this region, and photochemical decay of PAHs after emission, could explain the WQS data distribution on the plot. This agrees well with the results reported by Gao et al. (2012) at the same site. It should be noticed that Zhujiang Power Plant, which is the biggest electricity production base in Guangzhou, is about 10 km upwind of the sampling site. This coal–fired power plant may contribute greatly to the parent PAH levels at WQS, making the PAH concentrations at this rural site comparable with urban sites.

Sources and formation pathways of PAH derivatives. Specific compounds and ratios were used for a preliminary evaluation of PAHs derivatives sources. The ratio of 2NF/1NP has been extensively used to investigate the relative contribution of primary and secondary sources of NPAHs (Zielinska et al., 1989), whereas the ratio of 2NF/2NP is traditionally applied to explore the importance of gaseous phase NPAHs formation initiated by daytime OH radical or nighttime NO_3 radical (Arey et al., 1989; Atkinson and Arey, 1994). 2NF is the major NPAH product of the gaseous phase OH and NO_3 radical–initiated reaction of fluoranthene (Arey et al., 1986; Atkinson et al., 1987). 1NP is generally emitted from diesel powered engines (Nielsen, 1984), and could also be formed through the heterogeneous reactions of pyrene on the surface of particles, but only for a small proportion (Ringuet et al., 2012; Zimmermann et al., 2012). 2NP is the only nitropyrene formed through the reaction between Pyr and OH but not with NO_3 (Arey et al., 1986). Generally, 2NF/1NP less than 5 indicates a prevalence of primary emission; on the other hand, if this ratio is greater than 5, it is indicative of the importance of secondary formation. The ratio of 2NF/2NP close to 10 manifests the daytime OH initiated pathway, while the value over 100 suggests the dominance of the nighttime NO_3 initiated pathway (Arey et al., 1989; Atkinson and Arey, 1994).

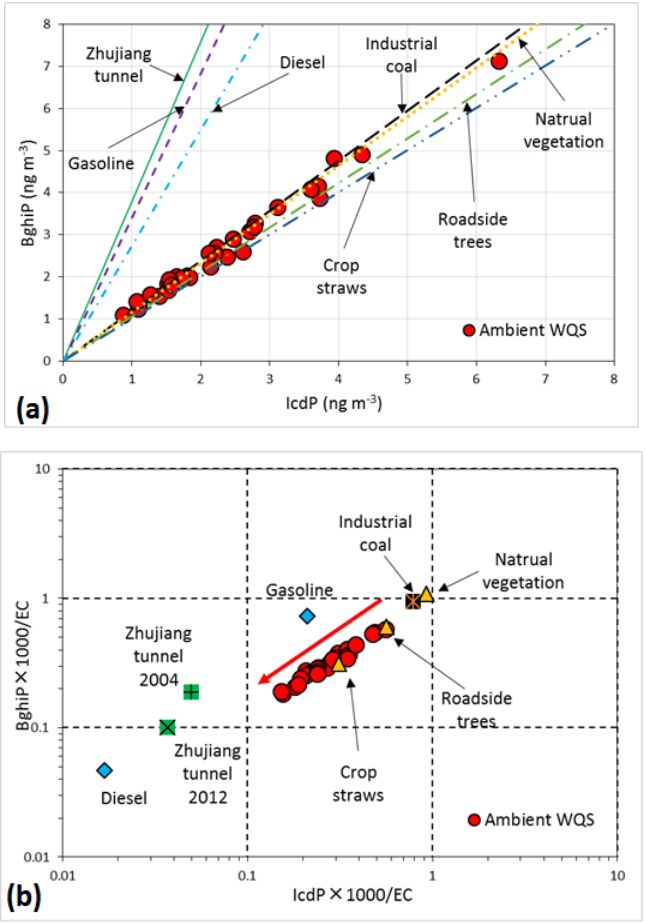

Figure 3. *BghiP vs IcdP:* ***(a)*** *Scatter plot of BghiP and IcdP concentrations in ambient WQS;* ***(b)*** *Ratio–to–ratio plot normalized by EC. Also shown in the plots are emission ratio curves for different sources including industrial coal combustion (Zhang et al., 2008), gasoline– and diesel–powered vehicular emissions (Zielinska et al., 1998), Zhujiang Tunnel 2004 (He et al., 2008), Zhujiang Tunnel 2012 (unpublished results), and biomass burning emissions (Wang, 2008).*

In this study, the ratio of 2NF/1NP ranged from 43.6 to 148, with an average value of 89.1, indicating a great contribution from secondary formation. Figure S3 (see the SM) shows the temporal variation of 2NF/1NP during the whole sampling period. The highest values of 2NF/1NP occurred on two hazy days (Dec 6th and Dec 23th). The highest TSP concentration throughout the entire sampling period appeared on Dec 6th, which was characterized with extremely low visibility (2.4 km), high RH (87.6%) and low wind speed. The hazy weather was unfavorable for the dispersion of contaminants, and this might have a positive impact on the secondary formation of NPAHs (Tan et al., 2009).

The average ratio of 2NF/2NP was 16.9 and the ratio values ranged from 8.63 to 33.6, indicating the contribution of both the daytime OH initiated and nighttime NO_3 initiated pathways in this region. The ratios were comparable with those measured in winter Baltimore (USA) (Bamford and Baker, 2003), Qingyuan (China) (Wei

et al., 2012), but were higher than ratios in samples collected in Athens (Greece) (Marino et al., 2000), and Beijing (China) (Wang et al., 2011). Generally, the contribution of the NO_3 initiated pathway is higher at remote sites, because at the sites with dense traffic, the concentration of NO_3 will be limited by NO, since NO reacts with and removes NO_3 and O_3, lowering the concentration of NO_3 radical (Reisen and Arey, 2005). For this reason, the 2NF/2NP ratio was found to be negatively correlated with NO (R=–0.727; p<0.01). However, the OH concentration in PRD region was (15–26)×10^6 molecules cm^{-3}, which were among the highest values reported for urban and suburban areas (Lu et al., 2012), suggesting OH reactions still might be the dominant formation pathway. Using 10 as the formation ratio for OH (R_{OH}) and 100 as the formation ratio for NO_3 (R_{NO3}), the contribution of OH reaction (α_{OH}) was estimated through the equation proposed by Feilberg et al. (2001):

$$\alpha_{OH}=(R_{obs}-R_{NO3})/(R_{OH}-R_{NO3}) \quad (5)$$

where, R_{obs} is the observed 2NF/2NP ratios. The calculated OH reaction contribution varied between 73.8% and 100%, with an average proportion of 92.6%. The results demonstrate clearly that gas–phase formation involving the OH radicals and parent compounds was the dominant photochemical pathway during the whole sampling period, and the contribution of the NO_3 pathway might be strengthened under specific conditions.

3.4. Inhalation risk assessment

The risk of cancer from exposing to the PAH mixtures was evaluated using the Relative Potency Factor (*RPF*) approach based on the U.S. EPA (U.S. EPA, 2010). Benzo[*a*]pyrene (BaP) was set as the index compound (*RPF*=1) and BaP equivalent (BaPeq) concentration of individual PAHs was calculated by multiplying their concentrations by their *RPF*. The inhalation cancer risk for the PAH mixture was then estimated by multiplying the total BaPeq concentration by the unit risk BaP (UR_{BaP}) (Jia et al., 2011), which is equal to 1.1×10^{-3} (μg m^3)$^{-1}$, according to OEHHA (2005). The equation for the cancer risk calculation is as follows:

$$Cancer\ Risk=\Sigma(C_{PAHi}\times RPF_i)\times UR_{BaP} \quad (6)$$

where, C_{PAHi} is the concentration of the i^{th} individual PAH, and RPF_i is the RPF of the i^{th} individual PAH.

A total of 18 carcinogenic compounds (12 PAHs and 6 NPAHs) were included in the estimation (Table 2). Potency Equivalency Factors (*PEF*) were applied in the calculation (OEHHA, 2005) for all 6 NPAHs due to the unavailability of RPF values. The rest of the compounds measured in this study were not assessed for their risk since corresponding reference values were not available. The estimated total lifetime excess inhalation cancer risk was 1.12×10^{-5} for these 18 compounds. The 6 NPAHs contributed 3.5% to the total toxicity, although they only accounted for 0.7% of the total mass of the 18 compounds. Most of the toxicity was ascribed to the particulate phase, reaching up to 87.3% on average. Albinet et al. (2008) reported that the risk associated to NPAHs could be as high as 20% of the total risk, depending on the type of site, its location and the season, which may influence the contribution of atmospheric NPAHs formation. In this study, the concentrations of parent PAHs were several times higher than those reported by Albinet et al. (2008), thus reduced the relative risk proportion of NPAHs. On the whole, the risk induced by PAH derivatives should not be neglected, and more research is required to better understand and control their effect on human health.

Table 2. *BaP equivalent concentrations and excess inhalation cancer risks of individual PAHs and their derivatives*

	Compounds	RPF [a]	BaPeq				Excess Cancer Risk
			Particle	Gas	Total	Particle (%)	
PAHs (ng m^{-3})	BaP	1	1.63	0.02	1.65	98.9	1.81x10^{-6}
	Ant	0	0.00	0.00	0.00		
	BaA	0.2	0.19	0.03	0.22	84.8	2.40x10^{-7}
	BbF	0.8	2.45	0.07	2.52	97.4	2.77x10^{-6}
	BghiP	0.009	0.02	1.02x10^{-4}	0.02	99.6	2.64x10^{-8}
	BkF	0.03	0.04	6.19x10^{-4}	0.04	98.4	4.26x10^{-8}
	Chr	0.1	0.23	0.10	0.32	70.3	3.53x10^{-7}
	DBahA	10	3.68	0.03	3.71	99.3	4.08x10^{-6}
	Fla	0.08	0.13	1.04	1.17	11.0	1.28x10^{-6}
	IcdP	0.07	0.16	8.12x10^{-4}	0.16	99.5	1.79x10^{-7}
	Phe	0	0.00	0.00	0.00		
	Pyr	0	0.00	0.00	0.00		
	ΣPAHs		8.53	1.28	9.81	87.0	1.08x10^{-5}
		PEF [b]					
NPAH (pg m^{-3})	1NP	0.1	1.66	0.04	1.70	97.7	1.87x10^{-9}
	4NP	0.1	1.78	0.09	1.88	95.2	2.06x10^{-9}
	1,6DNP	10	266	0.00	266	100	2.93x10^{-7}
	1,8DNP	1	44.6	0.00	44.6	100	4.91x10^{-8}
	6NChr	10	24.4	0.43	24.8	98.3	2.73x10^{-8}
	2NFl	0.01	1.67	9.93	11.6	14.4	1.28x10^{-8}
	ΣNPAHs		341	10.5	351	97.0	3.86x10^{-7}
	Total compounds (ng m^{-3})		8.87	1.29	10.2	87.3	1.12x10^{-5}

[a] *Values taken from U.S. EPA (2010)*
[b] *Values taken from OEHHA (2005)*
See Table 1 for the abbreviations

4. Conclusions

During the sampling period, concentrations of NPAHs and OPAHs were one order of magnitude lower than their parent PAHs. The gas–to–particle partitioning of PAHs, NPAHs and OPAHs were significantly dependent on their MWs. High MW compounds were more associated with the particulate phase. The diagnostic ratio analysis showed that coal combustion or biomass burning were the possible dominant contributors to the parent PAHs in WQS. Secondary formation contributed more to the concentrations of NPAHs, and the gas phase reaction initiated by OH radical was the dominant formation pathway of NPAHs. Hazy condition might enhance the secondary formation of NPAHs. The overall cancer risk by inhalation risk assessment was 1.12×10^{-5}, with 18 compounds taken into the calculation. The NPAHs contributed 3.5% to the total toxicity with only 0.7% of total mass.

Acknowledgments

This work was supported by "Strategic Priority Research Program (B)'' of the Chinese Academy of Sciences (XDB05020205) and State Key Laboratory of Organic Geochemistry (SKLOG2013A01). We also thank the support from Youth Innovation Promotion Association, CAS. This is contribution from GIGCAS1793.

Supporting Material Available

Details of Reagents, Extraction procedure, and Instrumental analysis, Twenty four hour back trajectory of air masses reaching the sampling site during the sampling period (NOAA–HYSPLIT model) (Figure S1), Mass fraction of particulate PAHs, NPAHs and OPAHs according to their molecular weights in WQS (Figure S2), Temporal variation of ΣPAHs, ΣNPAHs and ΣOPAHs as well as the ratio of 2NF/1NP (Figure S3), Detection ions and retention times (min) of determined compounds (Table S1), Ambient parameters and concentrations of TSP, OC, EC and trace gases during the sampling period (Table S2), Correlation coefficients of PAHs, NPAHs and OPAHs with OC and EC (Table S3), Correlation matrix between target compounds with trace gases and meteorological parameters (Table S4). This information is available free of charge via the internet at http://www.atmospolres.com.

References

Albinet, A., Leoz–Garziandia, E., Budzinski, H., Villenave, E., Jaffrezo, J.L., 2008. Nitrated and oxygenated derivatives of polycyclic aromatic hydrocarbons in the ambient air of two French alpine valleys – Part 1: Concentrations, sources and gas/particle partitioning. *Atmospheric Environment* 42, 43–54.

Albinet, A., Leoz–Garziandia, E., Budzinski, H., Villenave, E., 2007. Polycyclic aromatic hydrocarbons (PAHs), nitrated PAHs and oxygenated PAHs in ambient air of the Marseilles area (South of France): Concentrations and sources. *Science of the Total Environment* 384, 280–292.

Andreou, G., Rapsomanikis, S., 2009. Polycyclic aromatic hydrocarbons and their oxygenated derivatives in the urban atmosphere of Athens. *Journal of Hazardous Materials* 172, 363–373.

Arey, J., Zielinska, B., Atkinson, R., Aschmann, S.M., 1989. Nitroarene products from the gas–phase reactions of volatile polycyclic aromatic–hydrocarbons with the OH radical and N_2O_5. *International Journal of Chemical Kinetics* 21, 775–799.

Arey, J., Zielinska, B., Atkinson, R., Winer, A.M., Ramdahl, T., Pitts, J.N., 1986. The formation of nitro–PAH from the gas–phase reactions of fluoranthene and pyrene with the OH radical in the presence of NO_x. *Atmospheric Environment* 20, 2339–2345.

Atkinson, R., Arey, J., 1994. Atmospheric chemistry of gas–phase polycyclic aromatic–hydrocarbons – formation of atmospheric mutagens. *Environmental Health Perspectives* 102, 117–126.

Atkinson, R., Arey, J., Zielinska, B., Pitts, J.N., Winer, A.M., 1987. Evidence for the transformation of polycyclic organic–matter in the atmosphere. *Atmospheric Environment* 21, 2261–2262.

ATSDR (Agency for Toxic Substances and Disease Registry), 1998. Toxicological Profile for Sulfur Dioxide, Atlanta, USA.

Bamford, H.A., Baker, J.E., 2003. Nitro–polycyclic aromatic hydrocarbon concentrations and sources in urban and suburban atmospheres of the Mid–Atlantic region. *Atmospheric Environment* 37, 2077–2091.

Bi, X.H., Sheng, G.Y., Peng, P., Chen, Y.J., Zhang, Z.Q., Fu, J.M., 2003. Distribution of particulate– and vapor–phase *n*–alkanes and polycyclic aromatic hydrocarbons in urban atmosphere of Guangzhou, China. *Atmospheric Environment* 37, 289–298.

Bidleman, T.F., 1988. Atmospheric processes – wet and dry deposition of organic–compounds are controlled by their vapor particle partitioning. *Environmental Science & Technology* 22, 361–367.

Callen, M.S., de la Cruz, M.T., Lopez, J.M., Murillo, R., Navarro, M.V., Mastral, A.M., 2008. Some inferences on the mechanism of atmospheric gas/particle partitioning of polycyclic aromatic hydrocarbons (PAH) at Zaragoza (Spain). *Chemosphere* 73, 1357–1365.

Chen, Y.J., Bi, X.H., Mai, B.X., Sheng, G.Y., Fu, J.M., 2004. Emission characterization of particulate/gaseous phases and size association for polycyclic aromatic hydrocarbons from residential coal combustion. *Fuel* 83, 781–790.

Chirico, R., Spezzano, P., Cataldi, D., 2007. Gas–particle partitioning of polycyclic aromatic hydrocarbons during the spring and summer in a suburban site near major traffic arteries. *Polycyclic Aromatic Compounds* 27, 401–423.

Cotham, W.E., Bidleman, T.F., 1995. Polycyclic aromatic–hydrocarbons and polychlorinated–biphenyls in air at an urban and a rural site near lake–Michigan. *Environmental Science & Technology* 29, 2782–2789.

EHC, 2003. Selected Nitro– and Nitro–Oxy–Polycyclic Aromatic Hydrocarbons, Hanover, Germany.

Fan, Z.H., Kamens, R.M., Hu, J.X., Zhang, J.B., McDow, S., 1996. Photostability of nitro polycyclic aromatic hydrocarbons on combustion soot particles in sunlight. *Environmental Science & Technology* 30, 1358–1364.

Fang, G.C., Wu, Y.S., Chen, M.H., Ho, T.T., Huang, S.H., Rau, J.Y., 2004. Polycyclic aromatic hydrocarbons study in Taichung, Taiwan, during 2002–2003. *Atmospheric Environment* 38, 3385–3391.

Feilberg, A., Poulsen, M.W.B., Nielsen, T., Skov, H., 2001. Occurrence and sources of particulate nitro–polycyclic aromatic hydrocarbons in ambient air in Denmark. *Atmospheric Environment* 35, 353–366.

Gaga, E.O., Ari, A., 2011. Gas–particle partitioning of polycyclic aromatic hydrocarbons (PAHs) in an urban traffic site in Eskisehir, Turkey. *Atmospheric Research* 99, 207–216.

Gao, B., Guo, H., Wang, X.M., Zhao, X.Y., Ling, Z.H., Zhang, Z., Liu, T.Y., 2012. Polycyclic aromatic hydrocarbons in $PM_{2.5}$ in Guangzhou, southern China: Spatiotemporal patterns and emission sources. *Journal of Hazardous Materials* 239, 78–87.

Goss, K.U., Schwarzenbach, R.P., 1998. Gas/solid and gas/liquid partitioning of organic compounds: Critical evaluation of the interpretation of equilibrium constants. *Environmental Science & Technology* 32, 2025–2032.

Harner, T., Bidleman, T.F., 1998. Octanol–air partition coefficient for describing particle/gas partitioning of aromatic compounds in urban air. *Environmental Science & Technology* 32, 1494–1502.

He, L.Y., Hu, M., Zhang, Y.H., Huang, X.F., Yao, T.T., 2008. Fine particle emissions from on–road vehicles in the Zhujiang Tunnel, China. *Environmental Science & Technology* 42, 4461–4466.

IARC (International Agency for Research on Cancer), 2012. A Review of Human Carcinogens: Some Chemicals in Industrial and Consumer Products, Food Contaminants and Flavourings, and Water Chlorination By–Products, Lyon, France.

Janhall, S., Jonsson, A.M., Molnar, P., Svensson, E.A., Hallquist, M., 2004. Size resolved traffic emission factors of submicrometer particles. *Atmospheric Environment* 38, 4331–4340.

Jia, Y.L., Stone, D., Wang, W.T., Schrlau, J., Tao, S., Simonich, S.L.M., 2011. Estimated reduction in cancer risk due to PAH exposures if source control measures during the 2008 Beijing Olympics were sustained. *Environmental Health Perspectives* 119, 815–820.

Kawanaka, Y., Matsumoto, E., Wang, N., Yun, S.J., Sakamoto, K., 2008. Contribution of nitrated polycyclic aromatic hydrocarbons to the mutagenicity of ultrafine particles in the roadside atmosphere. *Atmospheric Environment* 42, 7423–7428.

Kim, J.Y., Lee, J.Y., Kim, Y.P., Lee, S.B., Jin, H.C., Bae, G.N., 2012a. Seasonal characteristics of the gaseous and particulate PAHs at a roadside station in Seoul, Korea. *Atmospheric Research* 116, 142–150.

Kim, J.Y., Lee, J.Y., Choi, S.D., Kim, Y.P., Ghim, Y.S., 2012b. Gaseous and particulate polycyclic aromatic hydrocarbons at the Gosan background site in East Asia. *Atmospheric Environment* 49, 311–319.

Kojima, Y., Inazu, K., Hisamatsu, Y., Okochi, H., Baba, T., Nagoya, T., 2010. Influence of secondary formation on atmospheric occurrences of oxygenated polycyclic aromatic hydrocarbons in airborne particles. *Atmospheric Environment* 44, 2873–2880.

Lohmann, R., Lammel, G., 2004. Adsorptive and absorptive contributions to the gas–particle partitioning of polycyclic aromatic hydrocarbons: State of knowledge and recommended parametrization for modeling. *Environmental Science & Technology* 38, 3793–3803.

Lu, K.D., Rohrer, F., Holland, F., Fuchs, H., Bohn, B., Brauers, T., Chang, C.C., Haseler, R., Hu, M., Kita, K., Kondo, Y., Li, X., Lou, S.R., Nehr, S., Shao, M., Zeng, L.M., Wahner, A., Zhang, Y.H., Hofzumahaus, A., 2012. Observation and modelling of OH and HO_2 concentrations in the Pearl River Delta 2006: A missing OH source in a VOC rich atmosphere. *Atmospheric Chemistry and Physics* 12, 1541–1569.

Lundstedt, S., White, P.A., Lemieux, C.L., Lynes, K.D., Lambert, L.B., Oberg, L., Haglund, P., Tysklind, M., 2007. Sources, fate, and toxic hazards of oxygenated polycyclic aromatic hydrocarbons (PAHs) at PAH–contaminated sites. *Ambio* 36, 475–485.

Marino, F., Cecinato, A., Siskos, P.A., 2000. Nitro–PAH in ambient particulate matter in the atmosphere of Athens. *Chemosphere* 40, 533–537.

Nielsen, T., 1984. Reactivity of polycyclic aromatic hydrocarbons towards nitrating species. *Environmental Science & Technology* 18, 157–163.

Odabasi, M., Cetin, E., Sofuoglu, A., 2006. Determination of octanol–air partition coefficients and supercooled liquid vapor pressures of PAHs as a function of temperature: Application to gas–particle partitioning in an urban atmosphere. *Atmospheric Environment* 40, 6615–6625.

Odabasi, M., Vardar, N., Sofuoglu, A., Tasdemir, Y., Holsen, T.M., 1999. Polycyclic aromatic hydrocarbons (PAHs) in Chicago air. *Science of the Total Environment* 227, 57–67.

OEHHA (Office of Environmental Health Hazard Assessment), 2005. Air Toxics Hot Spots Program Risk Assessment Guidelines. Part II: Technical Support Document For Describing Available Cancer Potency Factors, California, USA.

Pankow, J.F., 2001. A consideration of the role of gas/particle partitioning in the deposition of nicotine and other tobacco smoke compounds in the respiratory tract. *Chemical Research in Toxicology* 14, 1465–1481.

Ravindra, K., Sokhi, R., Van Grieken, R., 2008. Atmospheric polycyclic aromatic hydrocarbons: Source attribution, emission factors and regulation. *Atmospheric Environment* 42, 2895–2921.

Reisen, F., Arey, J., 2005. Atmospheric reactions influence seasonal PAH and nitro–PAH concentrations in the Los Angeles basin. *Environmental Science & Technology* 39, 64–73.

Ringuet, J., Albinet, A., Leoz–Garziandia, E., Budzinski, H., Villenave, E., 2012. Reactivity of polycyclic aromatic compounds (PAHs, NPAHs and OPAHs) adsorbed on natural aerosol particles exposed to atmospheric oxidants. *Atmospheric Environment* 61, 15–22.

Robinson, A.L., Subramanian, R., Donahue, N.M., Bernardo–Bricker, A., Rogge, W.F., 2006. Source apportionment of molecular markers and organic aerosols–1. Polycyclic aromatic hydrocarbons and methodology for data visualization. *Environmental Science & Technology* 40, 7803–7810.

Sienra, M.D., Rosazza, N.G., 2006. Occurrence of nitro–polycyclic aromatic hydrocarbons in urban particulate matter PM_{10}. *Atmospheric Research* 81, 265–276.

Simcik, M.F., Franz, T.P., Zhang, H.X., Eisenreich, S.J., 1998. Gas–particle partitioning of PCBs and PAHs in the Chicago urban and adjacent coastal atmosphere: States of equilibrium. *Environmental Science & Technology* 32, 251–257.

Sklorz, M., Briede, J.J., Schnelle–Kreis, J., Liu, Y., Cyrys, J., de Kok, T.M., Zimmermann, R., 2007. Concentration of oxygenated polycyclic aromatic hydrocarbons and oxygen free radical formation from urban particulate matter. *Journal of Toxicology and Environmental Health–Part A–Current Issues* 70, 1866–1869.

SPARC, 2013. https://archemcalc.com/sparc/test/login.cfm, accessed in July 2013.

Tan, J.H., Duan, J.C., Chen, D.H., Wang, X.H., Guo, S.J., Bi, X.H., Sheng, G.Y., He, K.B., Fu, J.M., 2009. Chemical characteristics of haze during summer and winter in Guangzhou. *Atmospheric Research* 94, 238–245.

Tobiszewski, M., Namiesnik, J., 2012. PAH diagnostic ratios for the identification of pollution emission sources. *Environmental Pollution* 162, 110–119.

Turpin, B.J., Lim, H.J., 2001. Species contributions to $PM_{2.5}$ mass concentrations: Revisiting common assumptions for estimating organic mass. *Aerosol Science and Technology* 35, 602–610.

U.S. EPA (U.S. Environmental Protection Agency), 2010. Development of a Relative Potency Factor (RPF) Approach for Polycyclic Aromatic Hydrocarbon (PAH) Mixtures, Washington, DC, USA.

Wang, Z., 2008. Emission factors and molecular tracers from typical biomass burning in Guangzhou, Ph.D. Thesis, Graduate School of Chinese Academy of Sciences, China, 105 pages.

Wang, W.T., Jariyasopit, N., Schrlau, J., Jia, Y.L., Tao, S., Yu, T.W., Dashwood, R.H., Zhang, W., Wang, X.J., Simonich, S.L.M., 2011. Concentration and photochemistry of PAHs, NPAHs, and OPAHs and toxicity of $PM_{2.5}$ during the Beijing Olympic Games. *Environmental Science & Technology* 45, 6887–6895.

Watson, J.G., Fujita, E., Chow, J.C., Zielinska, B., 1998. Northern Front Range Air Quality Study Final Report, Desert Research Institute, Reno.

Wei, S.L., Huang, B., Liu, M., Bi, X.H., Ren, Z.F., Sheng, G.Y., Fu, J.M., 2012. Characterization of $PM_{2.5}$–bound nitrated and oxygenated PAHs in two industrial sites of South China. *Atmospheric Research* 109, 76–83.

Wilson, N.K., McCurdy, T.R., 1995. Concentrations and phase distributions of nitrated and oxygenated polycyclic aromatic–hydrocarbons in ambient air. *Atmospheric Environment* 29, 2575–2584.

Yamasaki, H., Kuwata, K., Miyamoto, H., 1982. Effects of ambient–temperature on aspects of airborne polycyclic aromatic–hydrocarbons. *Environmental Science & Technology* 16, 189–194.

Zhang, Y.X., Schauer, J.J., Zhang, Y.H., Zeng, L.M., Wei, Y.J., Liu, Y., Shao, M., 2008. Characteristics of particulate carbon emissions from real–world Chinese coal combustion. *Environmental Science & Technology* 42, 5068–5073.

Zielinska, B., McDonald, J., Hayes, T., Chow, J.C., Fujita, E.M., Watson, J.G., 1998. Northern Front Range Air Quality Study Final Report Volume B: Source Measurements, Desert Research Institute, Reno.

Zielinska, B., Arey, J., Atkinson, R., Winer, A.M., 1989. The nitroarenes of molecular weight–247 in ambient particulate samples collected in southern California. *Atmospheric Environment* 23, 223–229.

Zimmermann, K., Atkinson, R., Arey, J., Kojima, Y., Inazu, K., 2012. Isomer distributions of molecular weight 247 and 273 nitro–PAHs in ambient samples, NIST diesel SRM, and from radical–initiated chamber reactions. *Atmospheric Environment* 55, 431–439.